INFLUENCE OF GEOMETRICAL PARAMETERS ON THE DYNAMIC CHARACTERISTICS OF THIN VERTICAL CLAMPED-FREE CYLINDRICAL SHELL

by

Bernardo A. Lejano

ABSTRACT

Recently the demand to build bigger and taller cylindrical shell structures has increased. This is accompanied with susceptibility to earthquake and wind vibrations. Hence, the design of such structures must ensure safety against these dynamic loads. Dynamic performance of structures is reflected in the dynamic characteristics. A finite element program suitable for the evaluation of the dynamic characteristics of cylindrical shell was developed for a 640K personal computer. The influence of geometrical parameters on the dynamic characteristics of the cylindrical shell was investigated using the said computer program.

INTRODUCTION

As of today, thin vertical cylindrical shells have been constructed for various purposes and functions. They have been used for storage containers, towers, chimneys, and others.

In developing computer programs using the finite element method (FEM) for the analysis of cylindrical shell, the actual structure was replaced by an assemblage of ring elements whose displacements are defined by an approximate function. The element used is similar to the axisymmetric shell element described by Zienkiewicz (Ref. 13). Two-noded elements were used to discretize the longitudinal section and Fourier series to define the circumferential behavior of the cylinder. The finite elements were formulated with the basic assumption that the behavior of the shell conforms to Kirchoff's theory. It is assumed that the shell is isotropic, homogeneous, and elastic. The base of the cylindrical shell is assumed to be totally fixed to the foundation and free at the top arising to the name clamped-free cylindrical shell.

The study involves the behavior of natural frequencies and mode shapes as affected by various geometrical parameters such as the height-to-radius ratio (H/R), the thickness-to-radius ratio (t/R), and the slope of the side of the cylinder with respect to the vertical axis.

THEORETICAL CONSIDERATION

The dynamic characteristics of a structure is reflected in the natural frequencies and mode shapes. These can be determined by evaluating the equation of free vibration without damping of the structure. The non-trivial solution is given as:

$$[K]\{X\} = \omega^2 [M]\{X\} \qquad \text{(Eqn.1)}$$

where
$[M]$ = mass matrix of the structure
$[K]$ = stiffness matrix of the structure
$\{X\}$ = modal shape
ω = natural frequency

To solve this eigenvalue problem, the determination of K and M matrices is necessary and is accomplished by FEM. This is done by subdividing the cylinder into ring elements (Figure 1). Actually, the problem is 3-dimensional but due to the rotational symmetry considerable simplification can be attained. This is done by expressing the behavior of circumferential deformation in terms of Fourier series. If the shell thickness is constant the approach can be eventually reduced to 1-dimension.

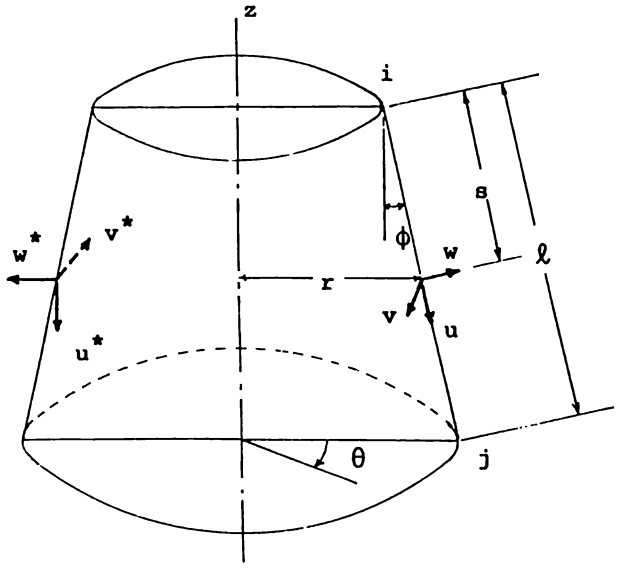

Fig.1 - Ring element.

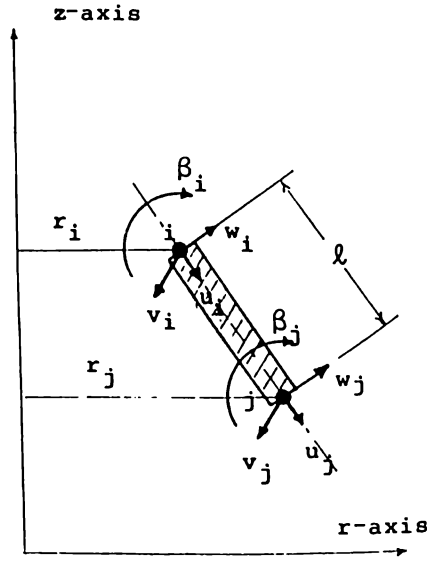

Fig.2 - Nodal displacement.

The displacement vector, {f}, is approximated using Fourier series as:

$$\{f\} = \sum_{n=0}^{\infty} \{fn\} = \sum_{n=0}^{\infty} [Tn]\ \{f\} \qquad \text{(Eqn.2)}$$

where n = integer number denoting Fourier series harmonic number

$\{f\} = [\, u, v, w \,]^T$ axial, circumferential and radial displacement, respectively

$\{fn\} = [\, un, vn, wn \,]^T$ displacement components corresponding to n

$\{\bar{f}\} = [\, \bar{u}, \bar{v}, \bar{w}, \,]^T$ displacement amplitudes

$$[Tn] = \begin{bmatrix} \text{Cos } n\,\theta & 0 & 0 \\ 0 & \text{Sin } n\,\theta & 0 \\ 0 & 0 & \text{Cos } n\,\theta \end{bmatrix}$$

θ_c = circumferential angle, as depicted in Figure 1

The displacement amplitudes can be expressed solely in terms of the mid-surface coordinate "s". The following are the assumed functions of the displacement amplitudes corresponding to the expected deformation of a 2-noded linear element.

$$\bar{u} = a_1 + a_2\, s \qquad \text{(linear axial deformation)}$$

$$\bar{v} = a_3 + a_4\, s \qquad \text{(linear circumferential deformation)} \qquad \text{(Eqn. 3)}$$

$$\bar{w} = a_5 + a_6 s + a_7\, s^2 + a_8 s^3 \qquad \text{(cubic radial deformation)}$$

The rotation about the s-axis is introduced to satisfy the continuity of elements.

$$\beta = dw/ds = a_6 + 2\, a_7 s + 3\, a_8 s^2$$

The coefficient a's are determined by applying the boundary conditions of the element. After the coefficients are determined, they are substituted back to Eqn.3. This results to the following equation:

$$\{\bar{f}\} = [N]\{x\} \qquad \text{(Eqn. 4)}$$

where $\{x\}$ = nodal displacement depicted in Figure 2
$[N]$ = shape function

Note that in Eqn.4, only the amplitude of the displacements are defined. The displacement corresponding to the harmonic "n" is:

$$\{fn\} = [Tn]\,[N]\,\{x\} \qquad \text{(Eqn.5)}$$

The strain-dsiplacement for axisymmetric thin shell is:

$$\{\varepsilon\} = \begin{Bmatrix} \varepsilon_{sn} \\ \varepsilon_{\theta n} \\ \gamma_{\theta sn} \\ \kappa_{sn} \\ \kappa_{\theta n} \\ \kappa_{n} \end{Bmatrix} = \begin{Bmatrix} -\frac{\partial un}{\partial s} \\ \frac{1}{r}\left(un\ Sin\phi + \frac{\partial vn}{\partial \theta} + wn\ Cos\phi\right) \\ \frac{1}{r}\left(\frac{\partial un}{\partial \theta} - vn\ Sin\phi + \frac{\partial vn}{\partial s}\right) \\ -\frac{\partial^2 wn}{\partial s^2} \\ -\frac{Sin\phi}{r}\left(\frac{\partial wn}{\partial s}\right) + \frac{1}{r^2}\left(\frac{\partial vn}{\partial \theta}\ Cos\phi - \frac{\partial^2 wn}{\partial \theta^2}\right) \\ \frac{1}{r}\left(\frac{\partial vn}{\partial s}\ Cos\phi - 2\frac{\partial^2 wn}{\partial s \partial \theta}\right) - \frac{2Sin\phi}{r^2}\left(vn\ Cos\phi - \frac{\partial wn}{\partial \theta}\right) \end{Bmatrix} \qquad \text{(Eqn.6)}$$

Substituting Eqn. 5 into Eqn. 6 yields:

$$\{\varepsilon n\} = [Tn]\,[B]\,\{x\} \qquad \text{(Eqn.7)}$$

where [B] is known as the strain-displacement transformation matrix. From basic finite element formulation for elastic problems, the element stiffness matrix of the present problem is computed as follows:

$$[Kn]e = \int [B]^T\,[Tn]^T[D]\,[Tn]\,[B]\,dVol \qquad \text{(Eqn.8)}$$

where dVol = t r d θ ds, t is the thickness of the shell

[D] = elasticity matrix taken from the stress-strain relation

Eqn.8 is further simplified by evaluating the integral involving the θ . The result is:

$$\text{for} \quad n > 0, \quad [Kn]e = \pi \int_0^{\ell} [B]^T [D] [B] \, t \, r \, ds \qquad \text{(Eqn.9)}$$

$$\text{for} \quad n = 0, \quad [K0]e = 2 \pi \int_0^{\ell} [B]^T [D] [B] \, t \, r \, ds$$

For n = 0, the problem is reduced to an axisymmetric loading case such that the displacement component v can be omitted since it is equal to zero.

The element mass matrix corresponding to harmonic "n" is evaluated as follows:

$$[Mn]e = \int p [Nn]^T [Nn] \, dVol \qquad \text{(Eqn.10)}$$

where p = mass density, [Nn] = [Tn] [N]

Similar to the stiffness matrix, the mass matrix is simplified.

$$[Mn]e = \pi p \int_0^{\ell} [N]^T [N] \, t \, r \, ds \qquad (\text{for } n > 0) \qquad \text{(Eqn. 11)}$$

$$[M0]e = 2\pi p \int_0^{\ell} [N]^T [N] \, t \, r \, d \, s \qquad (\text{for } n = 0)$$

Investigation of the integrals reveals that a 4-point Gauss-Legendre numerical integration is adequate to evaluate the integrals. The next step is to assemble the element matrices to form the structure matrices. Matrices assembly requires the matrices to be expressed in terms of the global coordinate system. This is achieved as follows:

$$[Kn^*]e = [\lambda]^T [Kn]e [\lambda] \; ; [Mn^*]e = [\lambda]^T [Mn]e [\lambda] \qquad \text{(Eqn.12)}$$

where [λ] is the coordinate transformation matrix. The asterisk (*) denotes globa orientation.

The next step is to assemble all element matrices to form the mass matrix and stiffnes matrix of the structure.

$$[Kn] = \bigwedge_{e=1}^{nel} [Kn^*]e \; ; \quad [Mn] = \bigwedge_{e=1}^{nel} [Mn^*]e \qquad \text{(Eqn.13)}$$

The symbol Λ denotes assembly.

The natural frequency and mode shapes can be obtained for each harmonic number by substituting the result of Eqn.13 into Eqn.1. In solving the eigenproblem, the subspace iteration method described by Bathe (Ref.2) was used.

VARIATION SHAPE OF CYLINDRICAL SHELL

A vibrating clamped-free cylindrical shell may be deformed in a variety of ways. However, the deformation can be distinctly identified in terms of the circumferential and axial mode shapes. When viewed from one end, the vibration of the shell may consist of any number of waves distributed around the circumference (Figure 3(a)). These circumferential waves are designated by numbers which correspond to the harmonic terms (n) of Fourier series. The circumferential wave corresponding to $n=0$ is the axisymmetric mode, $n=1$ is the swaying or flexural mode, $n=2$ is the ovalling mode, and $n>2$ are the breathing modes. Viewed from its side, the deformation of the cylinder consists of a number of waves distributed along the longitudinal axis (Figure 3(b). These longitudinal waves are denoted by m. The appearance of the axial wave resembles vibration deformation of a beam which have the same end condition as the shell. The combination of the circumferential waves and the axial waves (i.e. (m,n)) produces the vibration form of the cylinder for a given mode.

CONVERGENCE ANALYSIS

The convergence of the solution procedure was tested by solving the natural frequencies of a clamped-free cylindrical shell using different number of elements. The computed frequencies for the first 5 axial modes of circumferential wave number 1 are tabulated in Table 1. The results show good agreement to those obtained by Sen and Gould (Ref.10). It is observed that the natural frequencies converge monotonically to lower values as the number of elements is increased. Hence, the lowest value of each mode is deduced to be the closest to the true natural frequency. However, 10 elements is satisfactory for the dynamic analysis of clamped-free cylindrical shell, time-wise and memory-wise, and hence, was used in the subsequent analyses of the clamped-free cylindrical shell. It may be noticed also that higher axial modes are more affected by the number of elements used.

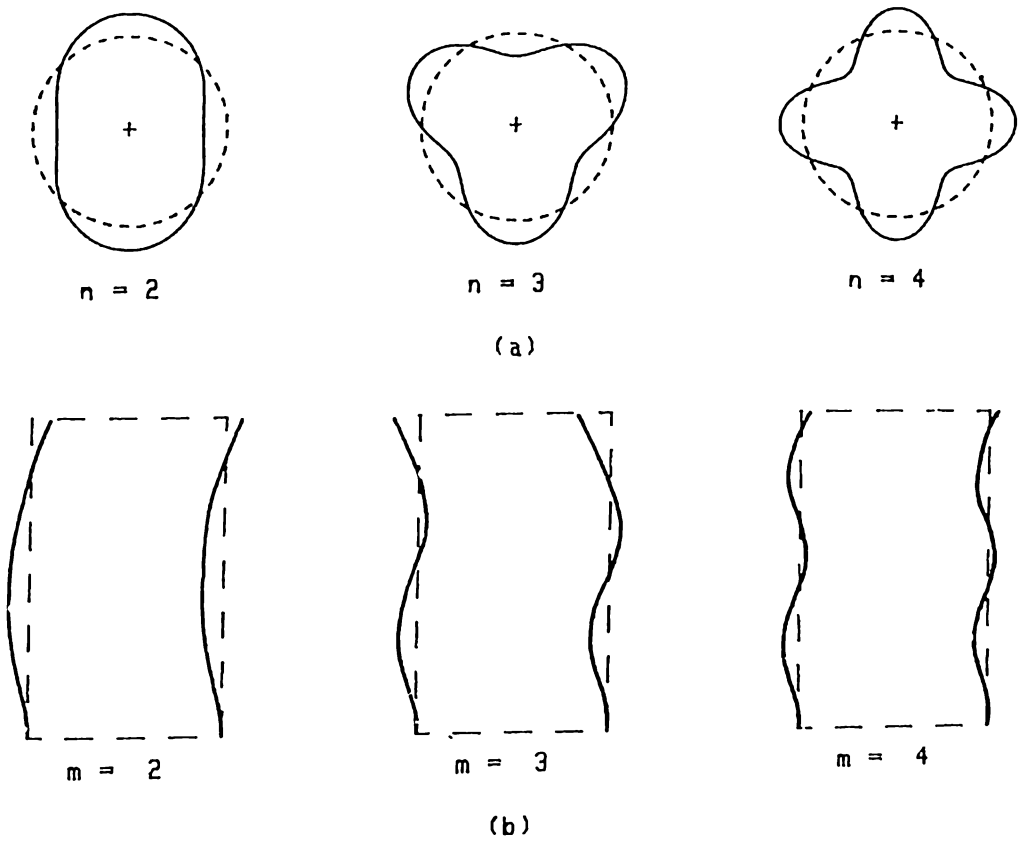

Figure 3-Vibration deformation shapes of cylindrical shell.

Table 1 - Computed natural frequencies (in Hz) for m = 1.
Data of the clamped-free cylindrical shell analyzed:
H = 22.68 cm, R = 10.16 cm, t = 0.10 cm,
E = 2,100,100 kg/cm^2, p = 8.019E-6 kg-sec^2/cm^4

No. of Elements	Time (sec.)	Axial Mode				
		m=1	m=2	m=3	m=4	m=5
5	398	2045.58	5520.15	7044.17	7687.82	7930.09
10	970	2034.89	5439.57	6968.67	7571.19	7766.48
15	1584	2032.93	5424.10	6953.98	7547.86	7547.86
20	1891	2032.32	5418.64	6949.06	7539.57	7719.86
25	2051	2032.07	5416.11	6946.83	7535.73	7714.08
30	2809	2031.94	5414.73	6945.62	7533.64	7710.92
35	3578	2031.87	5413.90	6944.90	7532.38	7709.00
40	3541	2031.83	5413.36	6944.43	7531.56	7707.75
45	3675	2031.80	5412.99	6944.11	7531.00	7706.90
50	5795	2031.77	5412.73	6943.88	7530.59	7706.28
Sen & Gould		2033	5431	6986	****	****

NATURAL FREQUENCY AND MODE SHAPES

Determination of the natural frequencies and mode shapes of the clamped-free cylindrical shell described in Table 1 was performed. The results are tabulated in Table 2 and graphed in Figure 4. The calculated frequencies are given for the first 5 axial modes (m) for various circumferential wave numbers (n) in the range from 0 to 16. For a particular value of n the natural frequency increases as the axial modes becomes higher. But for a particular mode m the natural frequency is distributed over n as a curve concave upwards as shown in Figure 4.

Table 3-Computed natural frequencies (in Hz) for various n.

n	m=1	m=2	m=3	m=4	m=5
0	5489.65	7966.39	8033.79	8078.48	8146.70
1	2034.89	5439.57	6968.67	7571.19	7766.49
2	985.13	3428.50	5797.73	6899.23	7456.60
3	567.79	2262.51	4410.47	5865.72	6767.17
4	489.60	1622.80	3387.78	4909.76	6031.28
5	622.62	1320.05	2716.14	4147.26	5362.51
6	863.49	1279.68	2335.61	3608.03	4824.39
7	1169.70	1434.24	2203.20	3289.90	4447.34
8	1529.57	1719.49	2279.17	3179.76	4242.28
9	1939.85	2092.64	2517.45	3255.49	4207.11
10	2399.51	2532.73	2875.70	3487.40	4329.61
11	2908.16	3030.41	3324.09	3844.87	4590.92
12	3465.65	3581.45	3844.80	4302.53	4970.40
13	4071.89	4183.78	4427.84	4842.26	5449.44
14	4726.85	4836.32	5067.72	5452.16	6013.30
15	5430.50	5538.48	5761.29	6124.68	6651.16

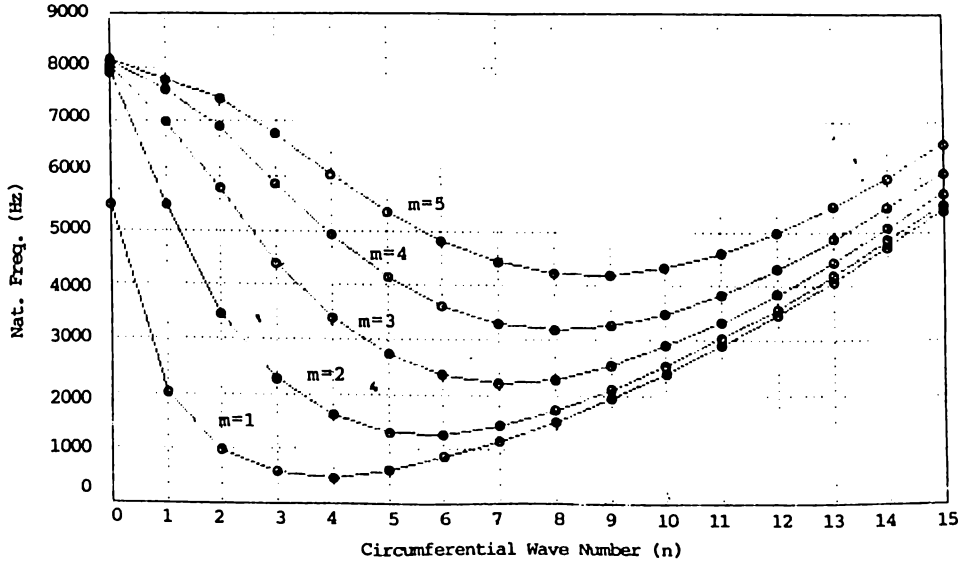

Fig. 4 - Natural frequency distribution with respect to n.

For the cylinder investigated, the lowest natural frequency or fundamental frequency occurs at the combination of m=1 and n=4. The fundamental frequency occured at a wavier circumferential deformation. Another phenomenon observed is that as m increases, the value of n corresponding to the minimum frequency also increases. In Figure 4 the minimum frequency for each axial mode are: (m,n)=(1,4), (m,n)=(2,6), (m,n)=(3,7), and so on. Note that frequencies for non-integer values of n have no physical significance. Based on the results, it may be deduced that it is possible for two modes to have identical natural frequency.

Presented in Figure 5 are some of the 3-dimensional graphical representation of the mode shapes of the cylinder. The 3-dimensional plot of the mode shapes was done by combining the shape of the circumferential wave and the axial mode shape. The shapes becomes complex as the natural frequency becomes higher. "Dimples" appear at combination of higher n and higher m. In general, the radial displacement, w, dominates the mode shapes. This is a typical characteristic of shells.

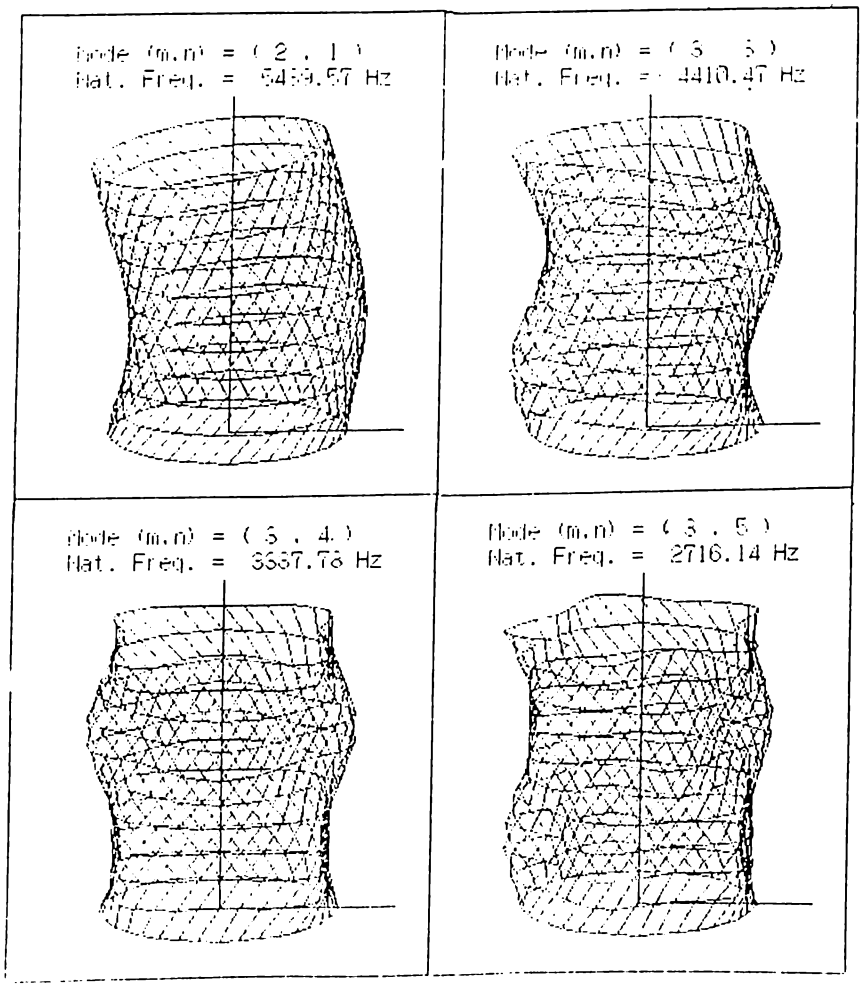

Fig. 5 Three-dimensional mode shapes.

INFLUENCE OF THICKNESS-TO-RADIUS RATIO

The effect of t/R was analyzed by calculating the first 5 natural frequencies of a clamped-free cylindrical shells having different t/R ranging from 0.01 to 0.05. The other parameters were fixed; R = 10, H/R = 1, and Poisson's ratio = 0.15. The results are graphed per circumferential wave number as shown in Figure 6.

A general characteristic observed is that the natural frequencies become higher as the thickness of the shell increases. This is attributed to a stiffer structure as the shell becomes thicker. The rate of increase at lower axial modes (m = 1 & 2) shows linear behavior. At higher circumferential wave numbers (n = 4 & 5), the rate of increase is greater. This means that as the shell becomes thicker, it becomes more unlikely that the lowest natural frequency will occur at a more wavy circumferential deformation. Hence, it can be said that the thinner the shell the higher the value of the circumferential wave number where the fundamental frequency will occur. It is also observed that the distribution of natural frequencies becomes closely spaced as the shell becomes thinner. This means that the thinner the cylindrical shell, the more it is susceptible to higher mode of vibrations.

INFLUENCE OF THICKNESS-TO-RADIUS RATIO

Clamped-free cylindrical shells of H/R in the range from 1 to 10 were investigated. The radius and Poisson's ratio were fixed to 10 and 0.15, respectively. The computed non-dimensional natural frequencies for t/R = 0.01 and varying H/R are presented in Figure 7. The results indicate the strong influence of H/R on the magnitude of the natural frequencies. The natural frequencies are found to decrease as H/R increases. They are significantly large at lower values of H/R. It is observed that the higher axial modes tend to approach the lower axial mode as H/R increases, thus, the natural frequencies become closely spaced at higher H/R. This means cylindrical shells with significantly large H/R are more susceptible to higher axial mode of vibration. It is also observed that the rate the natural frequencies become closely spaced is higher at higher values of n. Another observation is that the magnitude of the natural frequency corresponding to m = 1 is less affected by H/R at higher values of n. The graph for n = 0 exhibit a different behavior, however, the decrease in natural frequencies as H/R increases still holds true. The peculiar difference is that at H/R = 3 the higher axial modes became very closely spaced but separated one at a time and approached the lower modes as H/R was increased.

The occurrence of the fundamental frequency in the circumferential wave number domain as affected by H/R was investigated. Presented in Figure 8 is the graph of fundamental frequencies against H/R. The decrease in the fundamental frequency as H/R increases is very much pronounced here. The taller the cylinder, the lower its fundamental frequency. Also, it is observed that as H/R increases the fundamental frequency occurs at a lower value of n (as reflected in the number in parenthesis). This means that shell characteristics (n > 1) is lost for

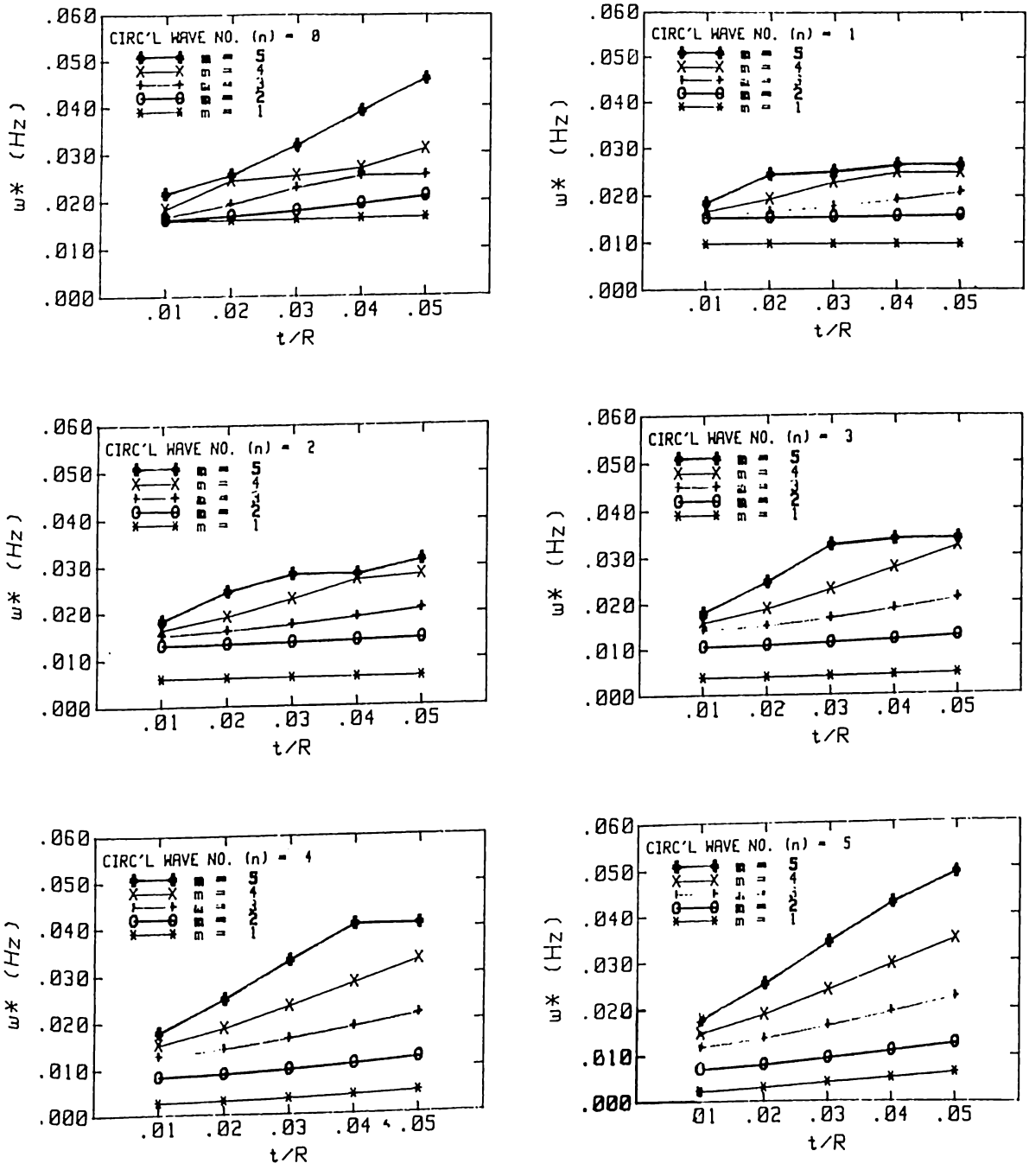

Fig. 6 - Effect Thickness-to-Radius Ratio (t/R)

(H/R=1, R=10, Poisson's ratio=0.15)

Note : $w^* = \text{Nat.freq.} / \sqrt{(E/\rho)}$

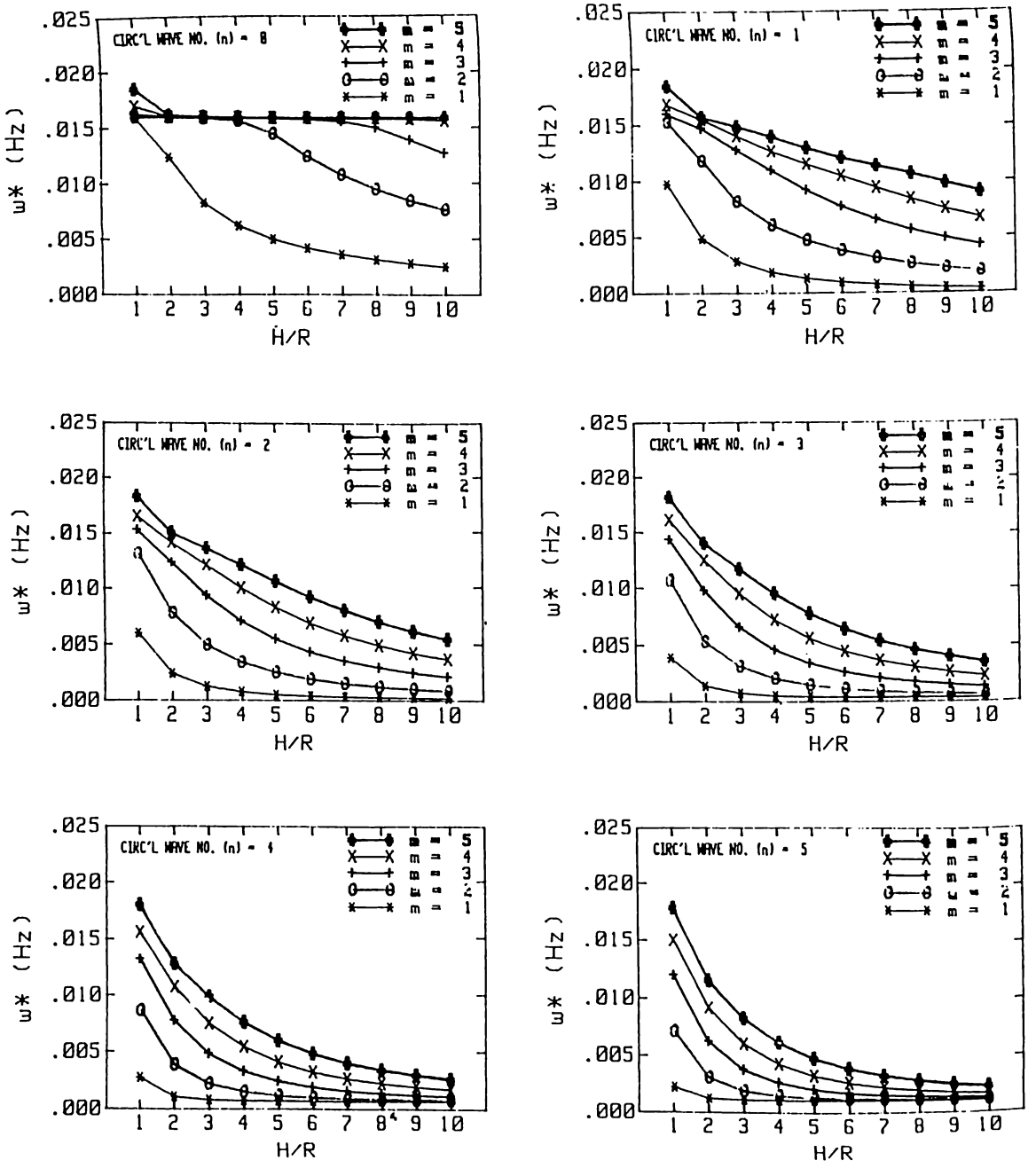

Fig. 7 - Effect Height-to-Radius (H/R)

(T/R=0.01, R=10, Poisson's ratio=0.15)

Note : $\omega^* = \text{Nat.freq.} / \sqrt{(E/\rho)}$

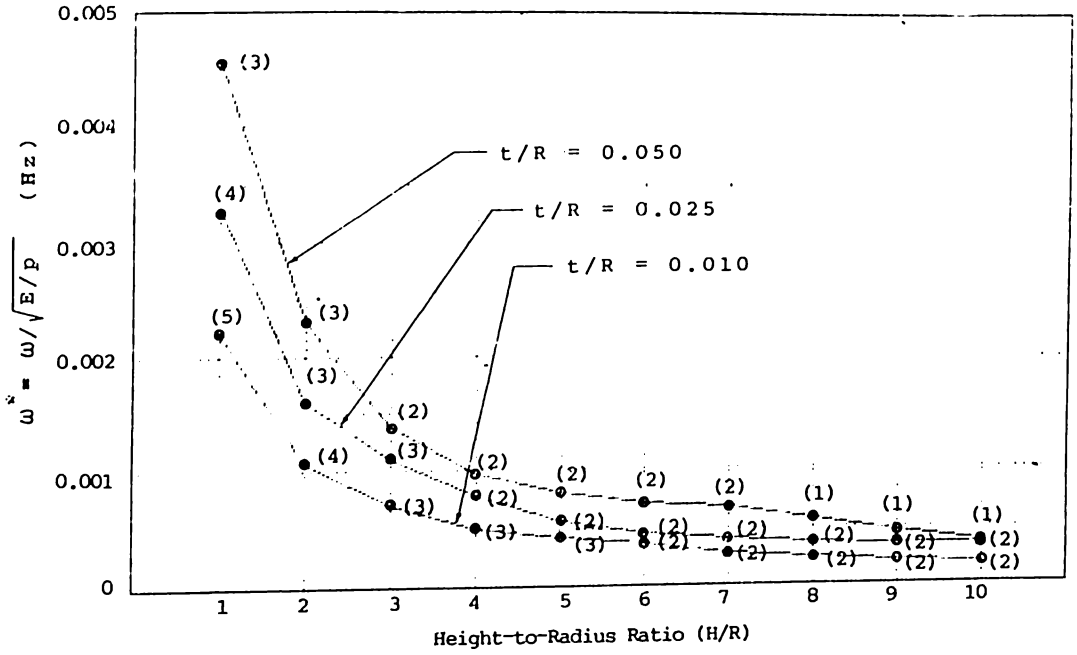

Fig. 8 - Effect of H/R on the Fundamental Frequency.

very tall cylinder, much more if the thickness of the shell is increased. The swaying mode will be dominant for very tall cylinder with thicker shell and the behavior would be like that of a cantilever beam.

INFLUENCE OF SLOPE

The slope of the side of the cylindrical shell with respect to the vertical axis was varied. The following parameters were fixed; H/R = 4, t/R = 0.01, base radius = 10, and Poisson's ratio = 0.15. Shown in Figure 9 is the result of this investigation. The slope is defined as ratio of the difference between the top and base radii against the height of the cylinder. The negative sign indicate that the cylinder is tapering upwards.

The dynamic behavior of the cylinder as affected by the slope is reflected in Figure 9. The natural frequencies decrease as the slope was changed from negative to positive. Lower circumferential wave numbers are seen to be more affected by the value of slope. Abrupt change in natural frequencies is observed at negative slopes, whereas it is smoothly decreasing at increasing positive slopes. The abrupt change seems to occur at higher circumferential wave number with smaller negative slopes.

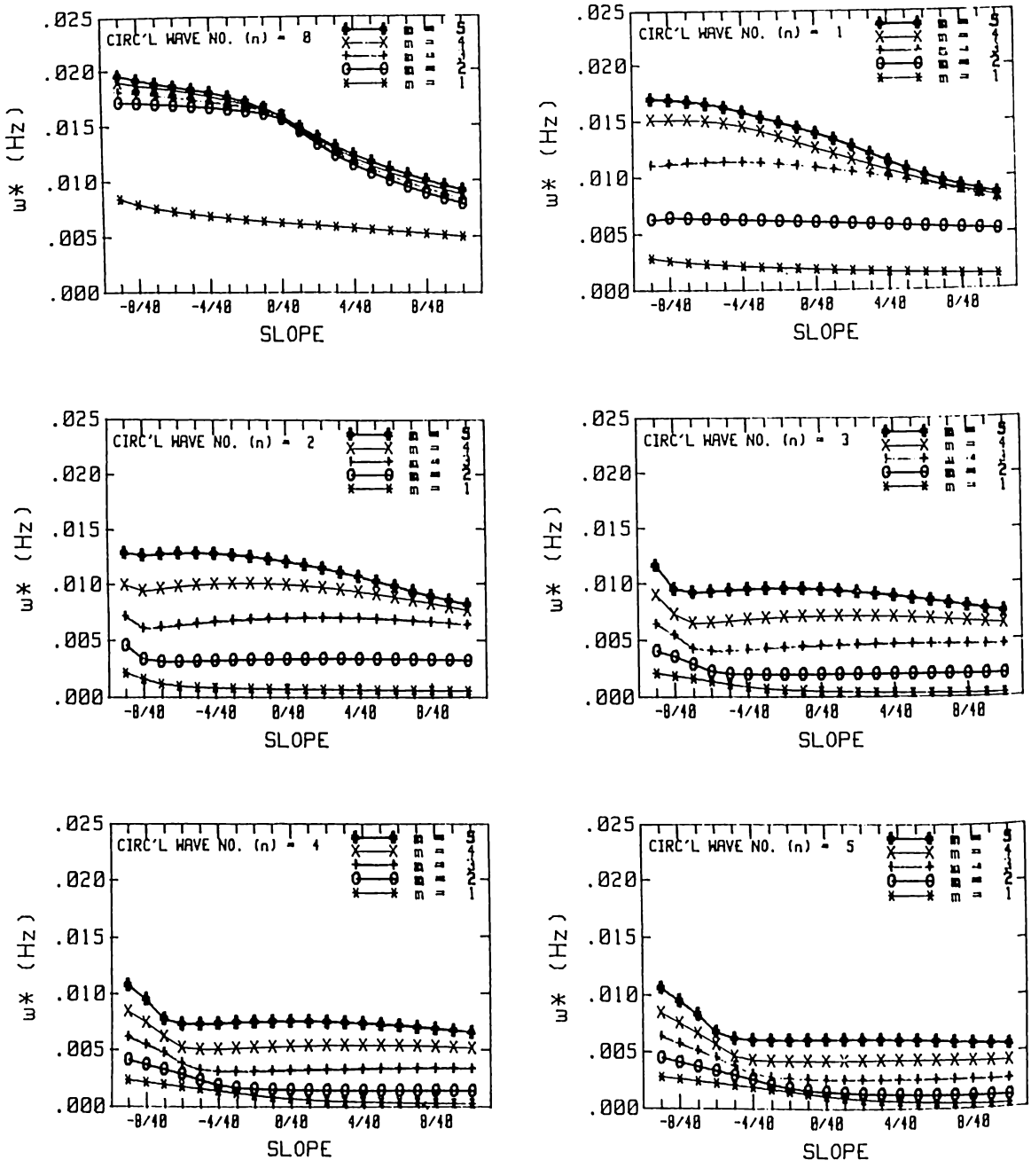

Fig. 9 - Effect Slope Variation

(H/R=4, t/R=0.01, R=10)

Note : w* = Nat.freq./ $\sqrt{(E/\rho)}$

CONCLUSION

A finite element program suitable for the evaluation of the dynamic characteristics of cylindrical shell was written in BASIC language and ran in a 640K personal computer. The element formulation was based from the works of Zienkiewicz (Ref. 13) for static analysis of axisymmetric shell. Reduction in computation effort was attained by expanding the circumferential displacements into Fourier series components. Subspace iteration method was used to solve the eigenvalue problem. The convergence was found to be monotonic and is approached from higher value.

The dynamic characteristics of a typical clamped-free cylindrical shell was investigated using the finite element program. The effects of slope, H/R, and t/R on the dynamic characteristics of the cylindrical shell were evaluated using the FEM program. The following conclusion may be made from the numerical investigation conducted: 1.) For each axial mode, the value of n at which the minimum natural frequency occurs is proportional to the value of m. 2.) In general the radial deformation, w, dominates the mode shapes. 3.) The natural frequencies decrease and become closely spaced as the cylindrical shell becomes thinner. 4.) The natural frequencies decrease and become closely spaced (especially at higher value of n) as H/R increases. Also, as the cylinder becomes shorter the lowest natural frequency occurs at higher value of n (i.e. at a wavier circumferential deformation). 5.) The natural frequencies can be increased by tapering the cylinder upwards.

ACKNOWLEDGEMENT

This study was carried out as part of the research program conducted by the Civil Engineering Division of the Integrated Research and Training Center (IRTC) at the Technological University of the Philippines (TUP). Some of the results presented here were based from thesis submitted by the author to the Graduate Division of the College of Engineering, University of the Philippines. The author expresses sincere gratitude to Dr. Salvador F. Reyes for his technical advice.

REFERENCES

1. Adelman, H.M., Catherines, D.S., and Walton, W.C., Accuracy of Modal Stress Calculations by the Finite Element Method, AIAA Journal, v.8, no. 3, 1970, pp. 462-468.

2. Bathe, K.J., Finite Element Procedures in Engineering Analysis, Prentice-Hall, New Jersey, 1982.

3. Forsberg, K., Influence of Boundary Conditions on the Modal Characteristics of Thin Cylindrical Shell, AIAA Journal, v.2, no. 12, 1964, pp.2150-2156.

4. Grafton P.E. and Strome, D.R., Analysis of Axisymmetrical Shell by the Direct Stiffness Method, AIAA Journal, v.1, no. 10, 1963, pp. 2342-2347.

5. Jones, R.E. and Strome, D.R., Direct Stiffness Method Analysis of Shells of Revolution Utilizing Curved Elements, AIAA Journal, v.4, no.9, 1966, pp.1519-1525.

6. Kraus, H., Thin Elastic Shells, John Wiley & Sons, Inc., New York, 1967, pp.289-314.

7. Leissa, A.W., Vibration of Shells, NASA SP-228, Washington D.C., 1973.

8. Lejano, B.A., Finite Element Method and Experimental Investigation of the Dynamic Characteristics of Vertical Cylindrical Shell, MSCE thesis, University of the Philippines, September, 1989.

9. Popov, E.P., Penzien, and Lu, Z., Finite Element Solution for Axisymmetric Shells, Journal of Engineering Mechanics Division ASCE, v.EM5, 1964, pp.119-145.

10. Sen, S.K. and Gould, P.L., Free Vibration of Shells of Revolution, Journal of Engineering Mechanics Division ASCE, v.100, no.EM2, 1974, pp. 283-303.

11. Sharma, C.B. and Johns, D.J., Natural Frequencies and Clamped Free Circular Cylindrical Shells, Journal of Sound and Vibration, v.21, no.3, 1972, pp.317-327.

12. Weingarten, V.I., Free Vibration of Thin Cylindrical Shells, AIAA Journal, v.2, no.4, 1964, pp. 717-722.

13. Zienkiewicz, O.C., The Finite Element Method in Structural and Continuum Mechanics, McGraw-Hill, London, 1967, pp. 138-147.